A Study on the Integration of a Sodium Borohydride ($NaBH_4$) Fuelled Hybrid System for a Small Inland Vessel

Ir. D. Lensing [a]

[a]Delft University of Technology, The Netherlands;

Synopsis

The use of fuel cells as a power source for propulsion can reduce the thermal and noise signatures of naval vessels drastically. However, safe and high energy-dense storage of hydrogen prevents this technology from being widely used. In this paper, a battery and hydrogen hybrid propulsion system fueled by $NaBH_4$ for a small inland vessel is designed and evaluated using MATLAB Simulink modelling. $NaBH_4$ is a hydrogen carrier that can react with water to produce pure hydrogen. The water can be produced on-board resulting in a high-density hydrogen storage option. In addition, the solid form of $NaBH_4$ is stable under atmospheric conditions, leading to a safe hydrogen storage option. The effectiveness of the system is studied by defining three operational profiles and using these profiles as inputs to size the energy storage components. To regulate the power between storage components, an energy management strategy (EMS) is implemented. Finally, different configurations are used to estimate the energy density of the system. The highest energy density is found at 1.2 kWh/ kg and 1.3 kWh/L of hydrogen for a 100-hour range using solid $NaBH_4$. The results implicate that using onboard produced water for the hydrolysis of $NaBH_4$ can enable a safe, and energy-dense hydrogen storage unique to the maritime industry.

Keywords: NaBH4, hydrogen generation system, PEMFC, Simulink, Energy Management System, alternative fuels

1 Introduction

Both naval and commercial vessels are increasingly interested in alternative fuels to reduce their carbon footprint and remain compliant with ECA and NECA regulations. When fuel cells are used instead of internal combustion engines, naval vessels also profit from highly reduced thermal and noise signatures. For this reason, and to increase the indiscretion ratio, hydrogen-fueled PEM fuel cells were already implemented in the U-212 submarines in 2002. However, conventional hydrogen storage solutions such as pressurised and liquid hydrogen solutions are large and limit the range capabilities of the vessel.

An alternative way of storing hydrogen is in the form of metal hydrides, figure 1 illustrates the volumetric and gravimetric energy density for various fuel options. Especially in terms of volumetric energy density, the metal hydrides show great potential over other carbon-free alternatives. One especially interesting hydride is Sodium Borohydride ($NaBH_4$). $NaBH_4$ is a complex metal hydride that stores hydrogen in a solid crystalline form and reacts with water to release hydrogen. The theoretical hydrogen storage capacity of the solid NaBH4 and its reactants is 10.8 wt%. However, if we exclude the water required for the hydrolysis and examine the hydrogen storage potential of pure, solid $NaBH_4$, a theoretical hydrogen storage capacity of 21.3 wt% is possible. Hydrogen has a typical lower heating value (LHV) of 33.3 kWh/kg, this results in a theoretical maximum LHV of 7.1 kWh/kg for $NaBH_4$. Solid $NaBH_4$ has a density of 1.07 kg/L so the theoretical maximum volumetric energy density is 7.6 kWh/L. Diesel has a higher LHV of 12.7 kWh/kg, however fuel cells are more efficient than diesel engines.

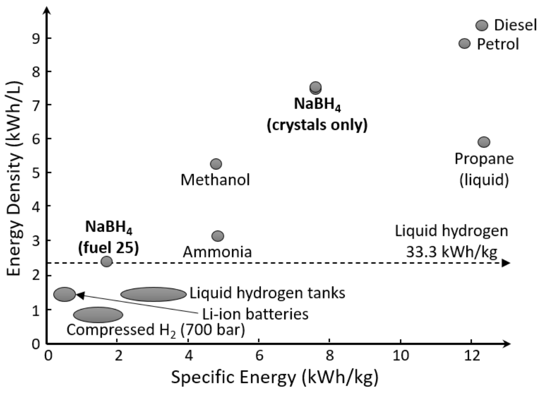

Figure 1: Gravimetric and volumetric energy densities for different fuels, modified to include $NaBH_4$ [1].

Authors' Biographies

Ir. D. Lensing is a junior researcher at the Delft University of Technology, he has a background in Mechanical and Maritime engineering, and researches the implementations of hydrogen systems in the maritime sector.

 https://doi.org/10.24868/issn.2515-818X.2020.060

The potential of energy-dense hydrogen storage and the inherent safety of $NaBH_4$ as a hydrogen carrier has encouraged several technological developments. The United States military experimented with $NaBH_4$ as fuel for Unmanned Aerial Vehicles (UAVs) and Unmanned Ground Vehicles (UGVs), realising a 2-7 times increase in specific energy compared to the existing battery systems [2]. In South Korea, further development of $NaBH_4$ as fuel for UAVs resulted in different prototypes, of which the most recent version derived a hydrogen storage capacity of 3.5 wt% by utilising a cartridge system [3][4][5]. Other research has implemented a batch reactor to reduce the amount of catalyst in the reactor and increase hydrogen generation efficiency [6].

The energy density of hydrogen storage systems is often compared to the United States Department of Energy's goals, as defined in table 1. The limiting factor for increasing the energy density for most applications of $NaBH_4$ is the water required for the reaction, which must be carried on-board. However, when designing a maritime application the water can be produced on-board by utilising reverse osmosis and water from the outside environment. The possibility of producing water from the outside environment could lead to a more energy-dense hydrogen storage solution.

The Port of Amsterdam (PoA) is developing a $NaBH_4$ fueled passenger vessel as part of the European H2SHIPS project to promote hydrogen applications in the maritime industry. This vessel is used as a case study for this paper. The main goals of this study are to design a $NaBH_4$ fueled propulsion system, to evaluate the effectiveness of $NaBH_4$ as a fuel, and to compare the estimated energy densities.

Table 1: DOE targets for hydrogen storage [7]

Storage parameters	Units	2020	2025	Ultimate
Gravimetric energy density	kWh/kg (kg H_2/kg system)	1.5(0.045)	1.8(0.055)	2.2(0.065)
Volumetric energy density	kWh/L (kg H_2/L system)	1.0(0.030)	1.3(0.040)	1.7(0.050)

2 The $NaBH_4$ Propulsion system

The application of a $NaBH_4$ as a fuel in the maritime industry has not been thoroughly researched. The maritime industry presents additional challenges regarding safety, power, and volume requirements. In contrast, it also introduces new potential by producing water on-board and recycling waste heat. This section will introduce some core concepts behind the $NaBH_4$ system and explore the implications for the maritime industry.

2.1 Hydrolysis reaction

The $NaBH_4$ reacts with water according to the hydrolysis reaction shown in equation 1. The reaction requires an excessive amount of water, indicated by the molar fraction y. The excess water increases the reaction speed but is mainly required to dissolve the reaction product $NaBO_2$ so the solution can be pumped out of the reactor. The mixture of $NaBO_2$ and water is called spent fuel and needs to be stored onboard the vessel. To maintain solubility, the molar fraction x_{NaBO_2} of the spent fuel solution should be no larger than 0.2 under ambient conditions [8].

$$NaBH_4 + (2+y)H_2O = 4H_2 + NaBO_2 \cdot yH_2O \tag{1}$$

The reaction is a spontaneous exothermic reaction with slow reaction kinetics. The reaction can be accelerated using either heat, a catalyst, or acid. The half-life of the reaction will be around 1 hour when using heat, 10 minutes with a catalyst, and under 1 minute with acid. Using acid will result in almost instantaneous hydrogen production, but at the expense of safety and energy density as highly reactive HCL acid must be stored on-board. In this paper, a system utilising a cobalt-based catalyst is examined to avoid the safety issues related to storing acid onboard the vessel.

The reaction rate as well as the reaction efficiency is also affected by the purity of the water [9]. Onboard this pure water can be produced by applying reverse osmosis to desalinate seawater and by utilising micro filters to achieve the desired purity. This also means that the reaction with contaminated water, such as seawater, will occur at a much slower rate.

2.2 Fuel types

The excess water required for equation 1 can either be stored together with the fuel or can be added later in the process. Equation 2 relates the excess water molar fraction y to the molar fraction x_{NaBO_2} in the spent fuel. The reaction requires 6 moles of water for every mole of $NaBH_4$ for a 0.2 molar fraction of x_{NaBO_2}. This equates to around 3 L of water per kg of $NaBH_4$.

$$y = \frac{1 - x_{NaBO_2}}{x_{NaBO_2}} \tag{2}$$

 https://doi.org/10.24868/issn.2515-818X.2020.060

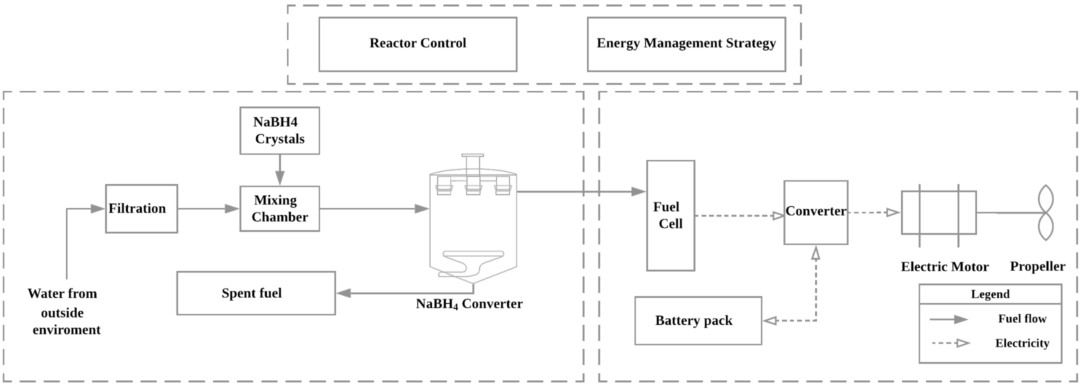

Figure 2: An overview of the required components for a $NaBH_4$ propulsion system using dry fuel.

The water can be either stored together with the $NaBH_4$ as fuel 25 or can be produced on board by filtering water from the outside environment. Fuel 25 is a reference to the 25 wt% of $NaBH_4$ in the solution. The fuel is easy to handle since the $NaBH_4$ is fully dissolved; however, the solution needs to be stabilised using NaOH to prevent hydrogen production in the storage tanks. For fuel 25, 5 wt% of NaOH is used to increase the pH value to 13-14, resulting in a half-life time between 42.6 and 426.3 days [10]. This will increase the stability of the fuel but will also significantly increase the weight and, possibly, cost.

Alternatively, dry fuel can be used. The fuel is stored in a solid crystalline form that dissolves in water, either produced onboard or stored. The energy cost for producing pure water on board is low, due mainly to desalinating seawater by using a reverse osmosis (RO) process. The power consumption of a RO process depends on the plant design and is estimated between 4-10 kWh per cubic metre of water [11]. Assuming 10 kWh, only 0.03 kWh per kg of $NaBH_4$ is required. Using dry fuel increases the complexity of the system but it can also dramatically increase the energy density if the water is produced onboard. This paper will compare both fuel options and compare the results based on the energy density of the complete system.

2.3 Fuel efficiency

The $NaBH_4$ system produces heat as a result of the exothermic reactions of the hydrolysis of $NaBH_4$ in the reactor and the reaction of H_2 in the PEM fuel cell. The heat of formation of the hydrolysis reaction 3 and reaction 4 can be used to create a Sankey diagram, illustrating the energy loss at different process steps. The industry-standard efficiency of 50% of the lower heating value (LHV) is assumed for a PEM fuel cell. LHV is assumed if the produced water remains in vapour form. If the water is allowed to condense, more energy will be released and the energy content is defined using the higher heating value (HHV), following equation 4. The fuel efficiency of one kg of $NaBH_4$ based on the higher heating value is illustrated using a Sankey diagram in figure 3. The reactor and the fuel cell operate on low temperatures of between 60-90°C. Consequently, the waste heat is difficult to convert into power, though it could be utilised in the HVAC systems onboard vessels.

$$NaBH_4 + 2H_2O(l) = 4H_2 + NaBO_2 \qquad \Delta H = -216.8 \quad kJ/mol \tag{3}$$
$$4H_2 + 2O_2 = 4H_2O(l) \qquad \Delta H = -1143.2 \quad kJ/mol \tag{4}$$

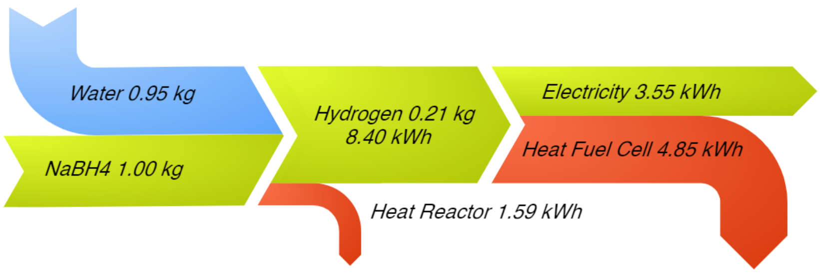

Figure 3: Sankey diagram for the energy loss at different stages for converting one kg of sodium borohydride to electricity.

 https://doi.org/10.24868/issn.2515-818X.2020.060

2.4 Safety

The safety risk of dry $NaBH_4$ stored on-board of a ship are similar to that of diesel oil. For example, the flashpoint and autoignition temperature of NaBH4 is 70 °and 220°C respectively, both higher than conventional diesel fuel. When ignited, however, NaBH4 will burn vigorously and needs to be extinguished using powder rather than water or foam. Since $NaBH_4$ can react with water, the effects of leakage in the fuel tanks could also create a possible safety risk. However, it is unclear if the reaction involving unfiltered water will happen fast enough to pose a problem. Further research and verification will be needed to properly address all the safety risks of dry $NaBH_4$ storage. Fuel 25, on the other hand, is stabilised using NaOH creating a very basic solution that prevents the hydrolysis reaction from taking place. NaBH4 itself is non-corrosive, however, when it reacts with water caustic soda (NaOH) can be formed. This substance is extremely corrosive but the formation chance is low and only happens in the reactor. The spent fuel product $NaBO_2$ is rather safe to store and the substance is non-flammable and non-corrosive. Only when extremely heated, in case of a fire for example, a toxic boron gas can be formed.

3 Simulation method

The implementation of a $NaBH_4$ system for propulsion onboard the Port of Amsterdam (PoA) vessel is evaluated using a MATLAB Simulink model. Figure 4 introduces a schematic overview of the Simulink model used. This section will elaborate on the various subsystems and how they are modelled.

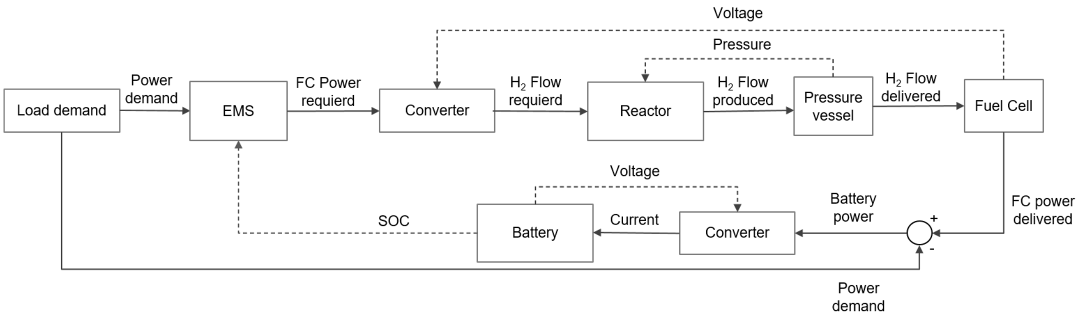

Figure 4: Schematic overview of the Simulink model

3.1 Load demand

The vessel currently used by the Port of Amsterdam (PoA) will be replaced with a similar but larger vessel. The new PoA vessel will be 20 metres in length instead of the current vessel's 15 metres. The enlarged vessel will have a similar design, thus the form factors such as block and prism coefficients are assumed constant. The design information for both the current and new PoA vessels, as given in table 2, can be used together with the Holtrop and Mennen method to calculate the resistance for both vessels.

Table 2: The characteristics of the new and old PoA vessel used to determine resistance.

	Disp.	Lwl	Bwl	T	T_{aft}	C_b	C_p	S_w	D_p
Current PoA vessel	35.547 m^3	16.3 m	3.5 m	0.86 m	0.59 m	0.73	0.74	56.5 m^2	0.76 m
New PoA vessel	48.901 m^3	19.5 m	4.0 m	0.86 m	0.59 m	0.73	0.74	86.0 m^2	0.76 m

Measurements of the shaft power and speed were done on the current vessel to determine a load profile for three average day scenario's. The measurements are then scaled based on the current speed using the Holtrop and Mennen resistance calculations. Based on the measurements and the design requirements, three scenarios are formulated to determine three operational profiles:

A. A tour through the city canals of Amsterdam. The ship sails mostly at low speeds with occasional high load demand for manoeuvring. The duration of the scenario is 5 hours.

B. The vessel visits the harbour for commercial purposes, sailing at moderate to high speed. The duration of the scenario is 5 hours.

C. The vessel is tested for the maximum range requirement and sails at moderate to high speeds. The duration of the scenario is 10 hours.

All three scenario's start with the vessel sailing from the docking area to the PoA headquarters followed by 15 minutes for embarking. All the scenario's end with 15 minutes for disembarking before returning to the docking area at full speed. Figure 5 shows the measurements and scaled measurements for the three operational profiles.

 https://doi.org/10.24868/issn.2515-818X.2020.060

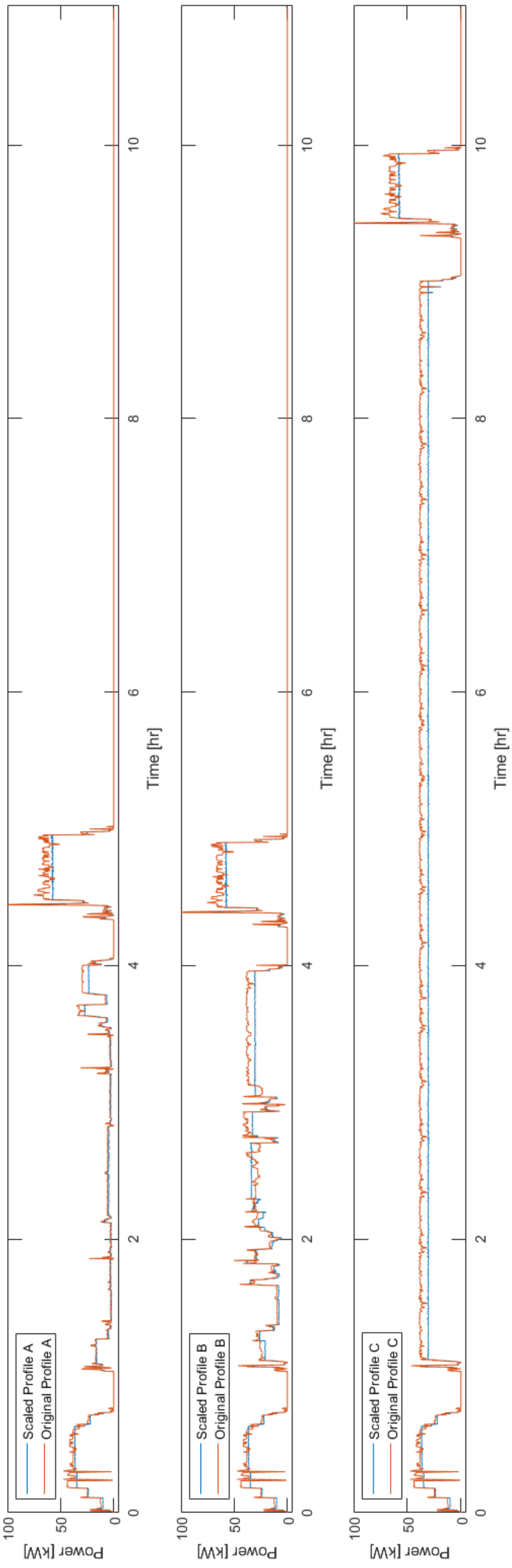

Figure 5: The three operational profiles used as input for the simulation, scaled for the new PoA vessel

https://doi.org/10.24868/issn.2515-818X.2020.060

3.2 Energy Management Strategy

The distribution of power between the fuel cell and the battery is determined by the Energy Management Strategy (EMS). The battery is the main power source with the fuel cell designed as a range extender. The fuel cell takes over part of the load from the battery either by recharging the battery during the trip or by supplying additional power during higher load requirements. The amount of power required from the fuel cell is a function of the State Of Charge (SOC) of the battery defined by the SOC_{high} and SOC_{low} in equation 5. Based on the current SOC of the battery, the fuel cell power is scaled from the minimum to the maximum fuel cell power between the two SOC settings. If the SOC is higher than the SOC_{high} value, the complete load is carried by the battery. If the fuel cell power determined by the EMS system is higher than the actual load requirement, the excess power is used to recharge the battery.

$$P_{FC}(SOC) = P_{FC,min} + \frac{SOC_{high} - SOC}{SOC_{high} - SOC_{low}}(P_{FC,max} - P_{FC,min}) \tag{5}$$

3.3 Reactor model

With a certain reaction temperature envelope, the hydrolysis reaction of $NaBH_4$ can be modelled using a first-order reaction described in equation 6. The half-life time of the reaction $t_{1/2}$ determines the $NaBH_4$ reaction rate d[A] and is a result of the reactor design and chosen catalyst. Besides the amount of starting reactant [A] and the type of catalyst used, other factors that influence the hydrogen production of the reaction include the temperature of the reaction, movement of reactants over the catalyst, surface area of the catalyst, and the presence of NaOH stabiliser in the solution. For the simulation, half-lives of 10 minutes and 5 minutes are evaluated based on the preliminary experience of the reactor prototype and the testing of a Co-B type catalyst.

$$-\frac{d[A]}{dt} = \frac{ln(2)}{t_{1/2}}[A] \tag{6}$$

The simulated reactor has an inner volume of 38 L and can be filled with 9 kg of $NaBH_4$ and the required amount of water. The NaBH4 is converted to hydrogen and the hydrogen is transported to the pressure vessel. If the pressure in the pressure vessel falls below 25 bar, the reactor discharges the produced spent fuel and any leftover $NaBH_4$. Finally, the reactor requires a 5 minute cleanse before a new batch can be injected. The control loop used for the reactor is illustrated in figure 6.

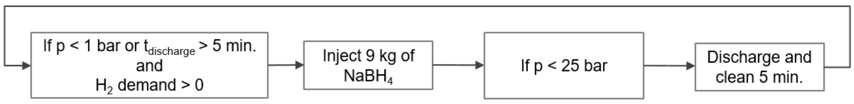

Figure 6: Control loop for the reactor model

3.4 Pressure vessel

A 200 L pressure vessel is installed after the hydrogen reactor to store the produced hydrogen and regulate the hydrogen flow to the fuel cell, serving as a buffer between the reactor and the fuel cell system. The error between hydrogen production and demand is accumulated in this vessel. The ideal gas law is assumed and the resulting pressure is used as an input for the reactor model.

3.5 Fuel cell and batteries

A proton exchange membrane (PEM) fuel cell is modelled using the MATLAB Simulink built-in models [11][12]. The product sheet of the Nedstack FCS 10-XXL module is used to simulate a 40 and 60 kW fuel cell. The minimum fuel consumption of the 10 kW module is 56 Nl/min compared to 120 Nl/min at maximum power, resulting in the $P_{FC,max}$ and $P_{FC,min}$ required for equation 5.

A Lithium-ion battery pack is also modelled using MATLAB Simulink built-in models [13]. The product sheet of the Valence U27-24XP lithium iron phosphate (LFP) battery module is used to simulate 50, 100 and 150 kWh battery packs. The battery pack has a maximum discharge rate of 2 C, meaning that the 50 kWh battery pack can provide 100 kW of power.

4 Results and discussion

This section provides and interprets the results of the simulations. First, the propulsion system without hydrogen production is considered, the EMS system is tuned, and a feasible sizing of battery and fuel cell systems is

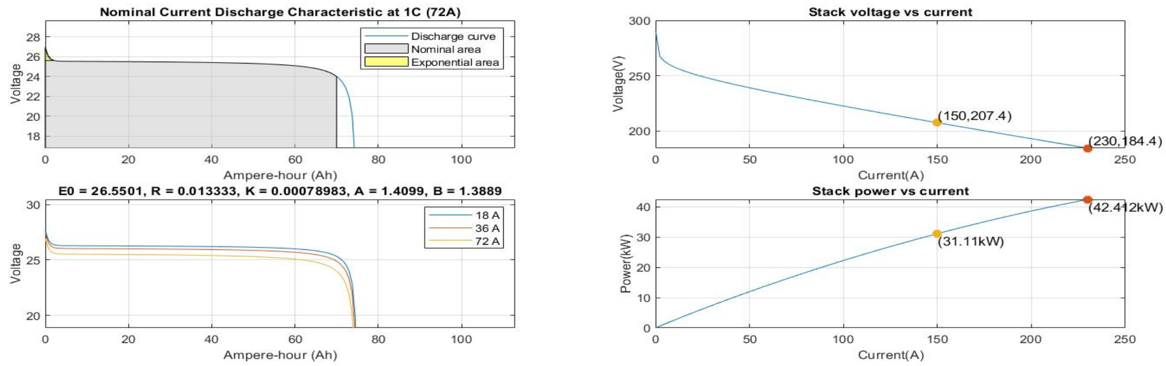

(a) Simulation of a single U27-24XP LFP battery module

(b) Simulation of the Nedstack MT-FCP-40 kW fuel cell

Figure 7: Fuel cell and battery simulation based on the product data sheets.

found. Then the complete system is simulated and the hydrogen supply and pressure inside the pressure vessel are evaluated. Using these results the energy density of the system is determined for different ranges using either fuel 25 or dry fuel.

4.1 Sizing of electrical systems and EMS settings

In table 3, four electrical system configurations are evaluated, configuration four has an additional 'manual override' allowing for the captain to decide to sail on purely batteries for short trips. Five criteria are used for the evaluation: hydrogen consumption, fuel cell efficiency, minimum SOC, maximum C-rate of the battery system, and the start/stop cycles of the fuel cell. Hydrogen consumption and fuel cell efficiency affect the operational costs of the vessel. The SOC rate and start/stop cycles affect the lifetime of the Li-ion batteries and fuel cell stack respectively. And the maximum C-rate indicates how much current a battery can discharge, normalized against the battery capacity. Exceeding the C-rate limit of a battery system can lead to overheating and must be avoided.

The SOC_{high} and SOC_{low} settings of the EMS system are tuned for the four configurations to achieve high minimum SOC and minimum start/stop cycles. It is found that the power output of the 40 kW fuel cell is not sufficient to carry the average load and is therefore activated early at 70% SOC. A 60 kW fuel cell can carry most of the load and can be activated at 40% SOC. The small battery pack of configuration 1 resulted in a higher hydrogen consumption and a C-rate of 2.6, exceeding the manufacturer's limit of 2. Furthermore, due to the high minimum power of the fuel cell, more start/stop cycles are observed compared to the 40 kW fuel cell. When using a 40 kW fuel cell, a larger battery pack of 150 kWh is required to achieve an acceptable minimum SOC of 29.74% after profile C. The added benefit of a large battery pack is that a 'battery only' mode is available and sufficient for small trips, increasing the redundancy of the design. It is found that configuration 4 is feasible and performs the best over the three profiles based on the five criteria.

Table 3: Simulation results for different configurations and EMS settings

		Configuration 1	Configuration 2	Configuration 3	Configuration 4
	Battery / Fuel cell	50 kWh / 60 kW	100 kWh / 40 kW	150 kWh / 40 kW	150 kWh / 40 kW
	EMS SOC settings	40-30	70-50	70-50	70-50 and 0
Profile A	H2 consumption [kg]	4.99	3.88	3.06	0
	Average FC efficiency	52.36%	52.46%	52.58%	0
	Min SOC	20.72%	54.56%	58.69%	27.95%
	C-rate max	2.62	1.03	1.02	1.02
	Start/stop	5	5	3	0
Profile B	H2 consumption [kg]	8.22	7.07	6.085	6.085
	Average FC efficiency	53.26%	51.09%	51.35%	51.35%
	Min SOC	23.26%	48.25%	52.84%	52.84%
	C-rate max	2.61	0.75	0.74	0.74
	Start/stop	5	2	1	1
Profile C	H2 consumption [kg]	22.39	20.61	19.59	19.59
	Average FC efficiency	52.32%	48.06%	48.28%	48.28%
	Min SOC	23.43%	15.00%	29.74%	29.74%
	C-rate max	2.61	0.67	0.67	0.67
	Start/stop	3	1	1	1

https://doi.org/10.24868/issn.2515-818X.2020.060

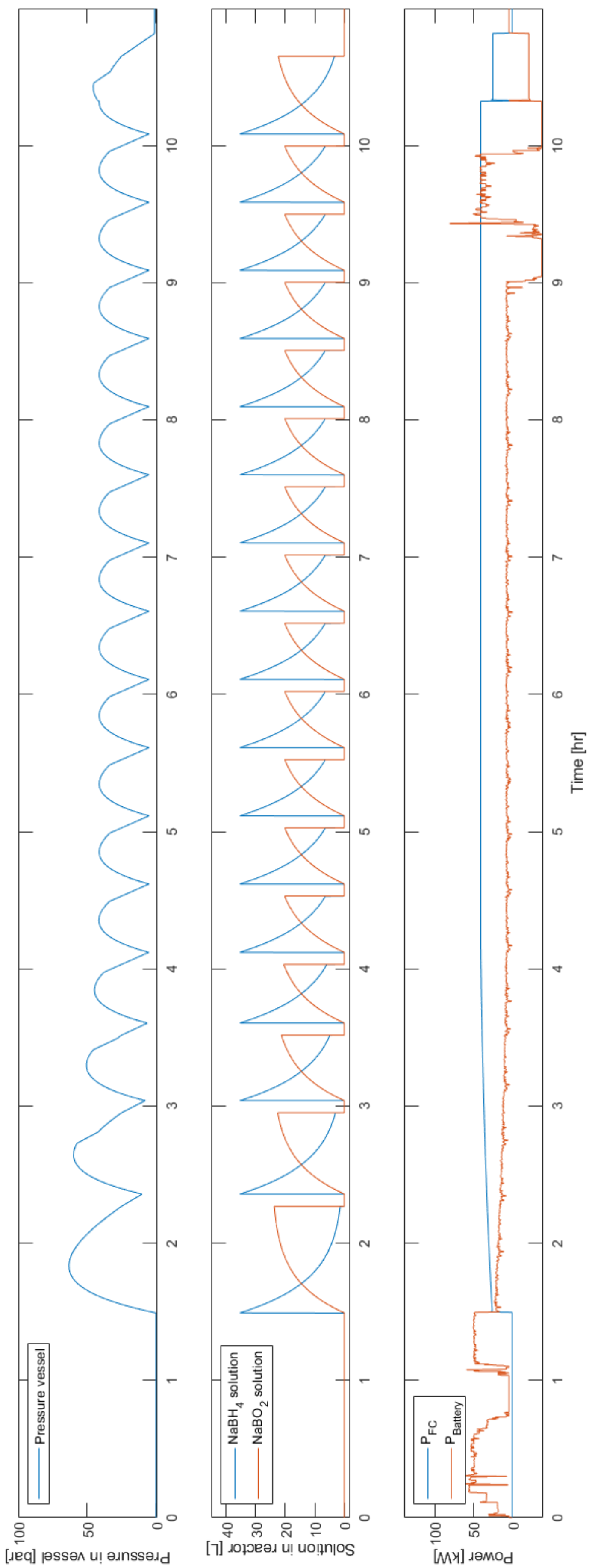

Figure 8: Simulation of the reactor and pressure vessel during operational profile C.

 https://doi.org/10.24868/issn.2515-818X.2020.060

4.2 Hydrogen supply

Figure 8 illustrates how the control loop provides continuous hydrogen flow during a simulation of operational profile three. The pressure vessel stores the excess hydrogen produced at the start of the reaction, as the reaction progresses it is producing less hydrogen and the pressure decreases. When the pressure falls below 25 bar, the reactor is discharged and cleaned and the remaining hydrogen is used until the reactor starts producing again. at the end of the operational profile, the leftover hydrogen is consumed at minimum fuel cell power and used to charge the batteries.

When the reactor discharges, the spent fuel is discharged together with any leftover $NaBH_4$, as can been seen in the second graph of figure 8. The discharge of unused $NaBH_4$ results in a percentage of lost $NaBH_4$. Fuel loss for a 10-minute half-life can be almost 16%, whereas fuel loss for a 5 minute half-life time is only 1%. The effects of a 10 minute or 5-minute half-lives are presented in table 4. The half-life of the reaction can be influenced by increasing the flow of the reactants and using more catalyst. It is crucial for the energy efficiency of the system that an acceptable half-life time is reached in the final design of the reactor. Another measure to reduce the fuel loss would be to increase the reactor inner volume and allow more $NaBH_4$ to be injected. This will increase the hydrogen that is stored in the pressure vessel, creating more time for the $NaBH_4$ to react.

Table 4: Simulation result for evaluating the hydrogen supply of the system.

	$t_{1/2}$ = 10 minutes			$t_{1/2}$= 5 minutes		
	Profile A	Profile B	Profile C	Profile A	Profile B	Profile C
NaBH4 Consumption [kg]	0.00	45.00	153.00	0.00	45.00	126.00
Spent Fuel [L]	0.00	114.9	352.10	0.00	122.90	341.40
Lost NaBH4 [%]	0.00%	6.76%	15.98%	0.00%	0.24 %	1.07%
Min SOC [%]	27.95%	50.77%	28.69%	27.95%	50.81%	28.70
Start/ Stop Cycles FC	0	2	2	0	2	2

4.3 Energy densities

The required size for the fuel and spent fuel tanks can be determined from table 4. In table 5 this information is used to estimate the system energy densities. The system for hydrogen storage includes the components as listed in the table but does not include the fuel cells or batteries. The energy densities are calculated using the LHV values of hydrogen and assume complete conversion of $NaBH_4$.

The storage system is evaluated for dry fuel and fuel 25, as well as for a 10 and 100 hr range. For the 10 hour range, the energy densities of dry fuel and a fuel 25 systems are similar. The filters required for the dry fuel system are not sufficiently compensated for by the gains in the density of the dry fuel to observe a large difference in system densities. Still, the fuel 25 configuration has the lowest gravimetric energy density of 409 Wh/kg. If a 50% fuel cell efficiency is assumed, the gravimetric energy density at a minimum is comparable to that of the state-of-the-art lithium-ion batteries.

The energy densities are affected by the system components that do not store energy such as the reactor and hydrogen scrubber. The effects of these components have less impact as the range of the vessel increases. For a 100 hour configuration using dry fuel, the gravimetric energy density is estimated at 1.2 kWh/kg or 3.6 wt% of hydrogen storage. This is similar to a state-of-the-art acid-based $NaBH_4$ cartridge system that utilises a much higher spent fuel molar fraction x_{NaBO_2} [5].

Theoretically, the impact of the non-energy-storing components will become nearly irrelevant as the range increases further and the relative contribution of the high amount of stored energy increases. Eventually, the energy density will only be dictated by the storage of dry fuel and spent fuel. In this case, the theoretical maximum hydrogen storage capacity using dry fuel and spent fuel at x_{NaBO_2}= 0.2 is 4.3 wt%, just short of the 2020 DOE target of 4.5 wt%. This could be further increased with a higher molar fraction x_{NaBO_2} in the spent fuel.

The gravimetric energy density is important, however, in shipbuilding, the space requirements can often be more limiting than the weight. Therefore, the volumetric energy density is also an important factor. For dry fuel and a 100-hour range, the volumetric energy density is estimated at 1.3 kWh/L, exceeding the DOE target for 2025.

 https://doi.org/10.24868/issn.2515-818X.2020.060

Table 5: Estimation of energy densities of the hydrogen storage system.

System components	volume [L]	Weight [kg]	10 hr range		100 hr range	
			Dry fuel	Fuel 25	Dry fuel	Fuel 25
Reactor	720	650	1	1	1	1
UPW instalatie	250	60	1	0	1	0
Scrubber H2	375	300	1	1	1	1
Dry fuel storage	130	125	1	0	10	0
Fuel 25 storage	550	529	0	1	0	10
Spent fuel tank	350	494	1	1	10	10
500 bar hydrogen tank [200 L/6.5 kg]	421	195	1	1	1	1
Volumetric energy density Wh/L			394	367	1349	842
Gravimetric energy density Wh/kg			486	409	1197	778
Hydrogen storage capacity wt%			1.5	1.2	3.6	2.3

5 Conclusions and further research

By modelling a $NaBH_4$ system for the Port of Amsterdam port authority vessel, a hybrid system was developed that combines a 40 kW fuel cell with a 150 kWh lithium-ion battery pack. Providing a 10-hour range and enough battery power to allow for a 'battery only' mode during a 5-hour range with low power demand.

A control loop for the hydrogen reactor was introduced and the simulation of the hydrolysis reaction suggests that a near-complete reaction of the $NaBH_4$ fuel is possible when the half-life of the reaction is increased. Two main mechanics for increasing the half-life could be adding more catalyst and increasing the reactant flow over the catalyst. Further research into validating the reactor control mechanisms and evaluating the reaction's half-life time is recommended.

An estimation was made for the energy densities of the hydrogen storage system. Using fuel 25, a gravimetric energy density of 427 Wh/kg and a volumetric energy density of 355 Wh/L was found. The energy density increases drastically to 1.3 kWh/L and 1.2 kWh/kg if dry fuel is used and the range is extended. Moreover, a theoretical maximum of 4.3 wt% of hydrogen storage was found when a spent fuel solution with a 0.2 $NaBO_2$ molar fraction is used. Further research is recommended into the conditions necessary for increasing the molar fraction while maintaining a solution that could be safely transported using pumps without creating a blockage. Since the spent fuel solutions are safe to store, it could also replace ballast water systems on-board of certain ships. Further research into the effectiveness of this method could also help to create a more energy-dense solution. The energy efficiency of the regeneration process is another major factor for the viability for $NaBH_4$ as a fuel and requires more research to become cost-effective.

In conclusion, $NaBH_4$ provides a relative safe option for hydrogen storage that could provide energy-dense storage onboard vessels. The possibility of using filtered water to react with solid $NaBH_4$ particles creates an interesting opportunity for energy-dense hydrogen storage that is unique to the maritime industry. For naval vessels, electrical zero-emission propulsion can lead to reduced thermal and noise signatures. Furthermore, using an energy-dense storage system will result in a longer mission duration and more range compared to conventional battery and hydrogen solutions.

Acknowledgement

The author acknowledges the support of the Port of Amsterdam, MARIN and H2FUEL. The research and development for the hydrogen application presented in this paper are funded in part by the NWE Interreg H2SHIPS project.

References

[1] PP Edwards, VL Kuznetsov, and WIF David. Hydrogen energy. *Philosophical Transactions of the Royal Society A: Mathematical, Physical and Engineering Sciences*, 365(1853):1043–1056, 2007.

[2] Jeff Baldic, Paul Osenar, Nick Lauder, and Peter Launie. Fuel Cell systems for long duration electric UAVs and UGVs. *Defense Transformation and Net-Centric Systems 2010*, 7707(May):031–039, 2010.

[3] Kyunghwan Kim, Taegyu Kim, Kiseong Lee, and Sejin Kwon. Fuel cell system with sodium borohydride as hydrogen source for unmanned aerial vehicles. *Journal of Power Sources*, 196(21):9069–9075, 2011.

[4] Taegyu Kim. NaBH4 (sodium borohydride) hydrogen generator with a volume-exchange fuel tank for small unmanned aerial vehicles powered by a PEM (proton exchange membrane) fuel cell. *Energy*, 69:721–727, 2014.

[5] Soon-mo Kwon, Shinuang Kang, and Taegyu Kim. Development of NaBH4-Based Hydrogen Generator for Fuel Cell Unmanned Aerial Vehicles with Movable Fuel Cartridge. *Energy Procedia*, 158:1930–1935, 2019.

[6] Valentina G. Minkina, Stanislav I. Shabunya, Vladimir I. Kalinin, and Alevtina Smirnova. Hydrogen gen-

eration from sodium borohydride solutions for stationary applications. *International Journal of Hydrogen Energy*, 41(22):9227–9233, jun 2016.

[7] U.S. Department of Energy. Technical Targets for Onboard Hydrogen Storage for Light-Duty Vehicles. `https://www.energy.gov/eere/fuelcells/fuel-cell-technologies-office`, 2019. Accessed: 19-05-2020.

[8] Jérôme Andrieux, Laetitia Laversenne, Olesia Krol, Rodica Chiriac, Zeinab Bouajila, Richard Tenu, Jean Jacques Counioux, and Christelle Goutaudier. Revision of the NaBO2–H2O phase diagram for optimized yield in the H2 generation through NaBH4 hydrolysis. *international journal of hydrogen energy*, 37(7):5798–5810, 2012.

[9] Aslı Boran, Serdar Erkan, and Inci Eroglu. Hydrogen generation from solid state nabh4 by using fecl3 catalyst for portable proton exchange membrane fuel cell applications. *International Journal of Hydrogen Energy*, 44(34):18915–18926, 2019.

[10] Umit Bilge Demirci, O Akdim, Jérôme Andrieux, Julien Hannauer, Rita Chamoun, and Philippe Miele. Sodium borohydride hydrolysis as hydrogen generator: issues, state of the art and applicability upstream from a fuel cell. *Fuel Cells*, 10(3):335–350, 2010.

[11] Reza Dashtpour and Sarim N Al-zubaidy. Energy Efficient Reverse Osmosis Desalination Process. *International Journal of Enviromental Science and Development*, 3(4):339–345, 2012.

[12] Olivier Tremblay, Louis-A Dessaint, et al. A generic fuel cell model for the simulation of fuel cell vehicles. In *2009 IEEE Vehicle Power and Propulsion Conference*, pages 1722–1729. IEEE, 2009.

[13] Olivier Tremblay and Louis-A Dessaint. Experimental validation of a battery dynamic model for EV applications. *World electric vehicle journal*, 3(2):289–298, 2009.

A $NaBO_2$-H_2O Phase diagram

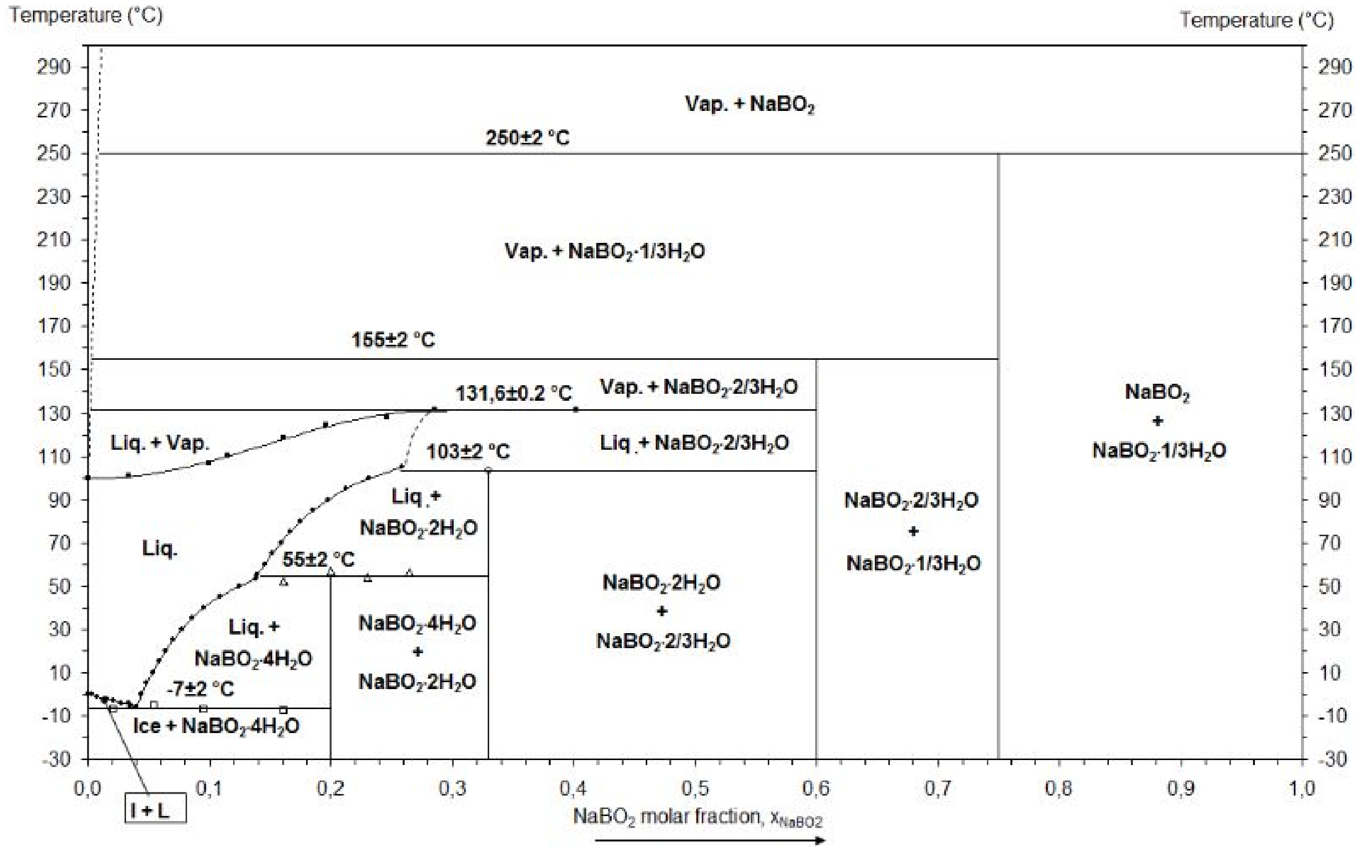

Figure 9: The phase diagram of $NaBO_2$ in water solutions [8].

https://doi.org/10.24868/issn.2515-818X.2020.060